Journal of Magnetic Resonance **141,** 52–61 (1999)
Article ID jmre.1999.1872, available online at http://www.idealibrary.com on IDEAL®

An *in Vivo* Evaluation of the Effects of Local Magnetic Susceptibility-Induced Gradients on Water Diffusion Measurements in Human Brain

C. A. Clark, G. J. Barker, and P. S. Tofts

NMR Research Unit, Institute of Neurology, University College London, Queen Square, London WC1N 3BG, United Kingdom

Received December 21, 1998; revised June 23, 1999

The effect of possible susceptibility-induced gradients on measurements of water diffusion along the transverse and longitudinal axes of white matter fibers in the brain was investigated *in vivo* at 1.5 T. Measurements obtained with sequences sensitive and insensitive, respectively, to susceptibility-induced gradients indicated that these gradients do not contribute significantly to diffusion anisotropy in brain white matter. Furthermore, diffusion measurements were unaffected by the presence of known susceptibility-induced gradients at the interface between the petrous bone and brain parenchyma. These results agree with those obtained on *in vitro* samples and appear to support the hypothesis that interactions between the diffusing water molecules and the cellular environment constitute the principal mechanism for diffusion anisotropy in brain white matter at 1.5 T. This, in turn, simplifies the interpretation of diffusion time-dependent measurements in terms of membrane separation and permeability.

Key Words: **diffusion; susceptibility; anisotropy; brain; MRI.**

INTRODUCTION

The diffusion of water molecules in central nervous system tissue may be monitored noninvasively using pulsed field gradient sensitized NMR techniques (*1–4*). Incoherent motion of proton spins along the direction of applied field gradients leads to imperfect refocussing of transverse magnetization and subsequent attenuation of the NMR signal. Quantification of the diffusion coefficient is possible by performing a series of experiments in which the sensitivity to diffusion (gradient *b* factor) is altered by modification of the pulsed gradient amplitudes and the NMR signals collected. The diffusion coefficient may be determined from a semilogarithmic plot of the attenuated NMR signal against the gradient *b* factor.

In brain white matter, water diffusion is anisotropic; the diffusion coefficient is dependent on the direction of the applied field gradient relative to the brain (*5–8*). Diffusion is more rapid along the direction of fiber tracts than across them. Although the exact mechanism for this phenomenon is not fully understood, the presence of cellular structures which differentially impede the progress of diffusing water molecules in certain directions is widely held to be an important contributory factor. The diffusion coefficient measured in tissue is referred to as an apparent diffusion coefficient (ADC) to reflect this modification of Einsteinian free diffusion as well as the effects of microcirculation (*9, 10*) and other physiological factors. More recently, the apparent diffusion tensor (ADT) has been used to describe tissue water diffusion, which embodies diffusion anisotropy in a single mathematical entity (*11, 12*). However, a more complete description may be provided from a series of diffusion time-dependent tensors. In this case the diffusion time, which is well defined in the pulsed field gradient sequence (*1*), is treated as a variable (*13–16*). In the short diffusion time regime few diffusing molecules interact with the surrounding cellular structures, diffusion anisotropy disappears, and the ADT is reduced to a scalar quantity. As the diffusion time increases so does the number of diffusing molecules that interact with the surrounding cellular structure, causing the ADC to be reduced relative to the free diffusion value in any particular direction. The rate of this reduction as a function of the diffusion time is considered to be reflective of the separation of the cellular structures and their permeability to water in a given direction (*17, 18*). In practice, this description of tissue water diffusion is limited by the resolution of the MRI technique available and the presence of additional signal modulation due to motion- and susceptibility-induced gradients. The effect of the latter phenomenon on measured tissue water diffusion *in vivo* and the implications of any such effects on the interpretation of white matter tissue structure form the main focus of this paper. The current theory regarding the effect of macroscopic and microscopic susceptibility-induced gradients on the measured ADC is briefly reviewed, followed by a description of experiments designed to detect the effects, if any, arising from these gradients in human brain.

THEORY

Macroscopic Susceptibility-Induced Gradients

Background gradients may arise from susceptibility variations in the sample or from poor magnetic field homogeneity. The use of a static, one-dimensional, macroscopic gradient during the collection of multiple spin echoes formed the basis of the first measurements of self-diffusion using NMR (*19*).

1090-7807/99 $30.00

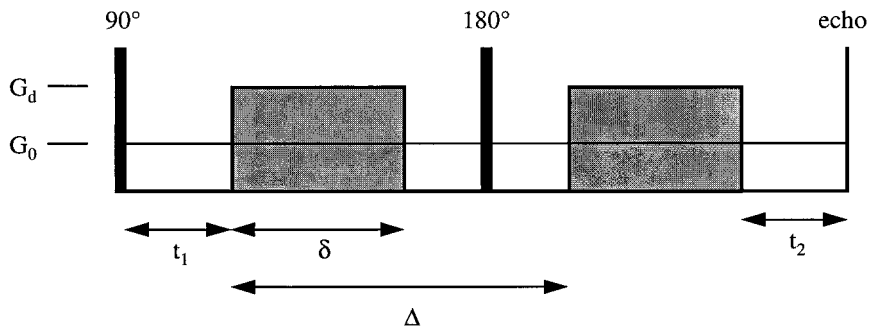

FIG. 1. The standard pulsed gradient spin echo (PGSE) sequence proposed by Stejskal and Tanner (*1*).

Stejskal and Tanner (*1*) considered the effect of a uniform background gradient on echo attenuation in a pulsed gradient spin echo (PGSE) experiment (as shown in Fig. 1) and described the echo attenuation in terms of the amplitude of the applied field gradient for diffusion sensitization **G** and the background gradient $\mathbf{G}_0$;

$$\ln\left[\frac{S(b)}{S(0)}\right] = -(b_d + b_{db})\mathrm{ADC}$$

where

$$b_d = \gamma^2\delta^2\left(\Delta - \frac{\delta}{3}\right)G^2$$

$$b_{db} = -\gamma^2\delta\left[(t_1^2 + t_2^2) + \delta(t_1 + t_2) + \frac{2\delta^2}{3} - \frac{(\mathrm{TE})^2}{2}\right]\mathbf{G}\cdot\mathbf{G_0} \qquad [1]$$

and where $S(b)$ and $S(0)$ are the NMR signals in the presence and absence of diffusion sensitization, respectively, b_d represents the gradient b factor due to the diffusion-sensitizing gradients, b_{db} is the diffusion and background gradient cross term, δ is the duration of the diffusion sensitising pulses, Δ is the separation between the leading edges of the diffusion sensitising pulses, t_1 is the time between the center of the 90° pulse and the start of the first diffusion pulse, and t_2 is the time from the end of the second diffusion pulse to the center of the spin echo.

It can be seen from Eq. [1] that components of the background gradient in the same direction as the diffusion-sensitizing gradients contribute to the cross term b_{db}. If this cross term is not accounted for, then an under- or overestimation of the ADC results, depending on whether the background gradient is antiparallel or parallel to the diffusion-sensitizing gradient, respectively. Equation [1] can be used to determine the relative error in the ADC determined from two NMR signals as a function of the background gradient amplitude (which is usually unaccounted for). The ADC can be calculated from Eq. [2] in which the denominator can be written (ignoring the imaging gradients), in terms of b_d and b_{db},

$$\mathrm{ADC} = \frac{\ln[S(0)/S(b)]}{b_d + b_{db}}. \qquad [2]$$

The relative error in the gradient b factor due to the noninclusion of the diffusion and background gradient cross term, b_{db}, may be defined as

$$\frac{\Delta b}{b} = \frac{b_{db}}{b_d + b_{db}} \times 100\%. \qquad [3]$$

The relative error in b can be related to the relative error in the ADC using propagation of errors

$$\frac{\Delta\mathrm{ADC}}{\mathrm{ADC}} = -\frac{\Delta b}{b}. \qquad [4]$$

Equation [1] also indicates that the cross term is dependent on δ, Δ, G, TE, t_1, and t_2. The magnitude of the cross term may be calculated for three cases; (i) using the optimal sequence parameters for maximal precision in the estimate of the water diffusion coefficient, (ii) using the optimal sequence parameters for maximal precision in the estimate of brain white matter ADC, and (iii) using parameters utilized for an experimental investigation of background gradient effects on the estimated ADC *in vivo*.

Maximal precision in the ADC estimated from two NMR signals collected with diffusion weighting $b_{min} = 0$ and b_{max} may be achieved by minimizing

$$\left(\frac{\sigma_{\mathrm{ADC}}}{\mathrm{ADC}}\right)^2 = \left(\frac{\sigma_{S_0}}{S_0}\right)^2\left[\frac{1 + \exp(2b_{max}\cdot\mathrm{ADC})}{(b_{max}\cdot\mathrm{ADC})^2}\right]\exp\left(\frac{2\mathrm{TE}}{T_2}\right), \qquad [5]$$

according to Prasad and Nalcioglu (*20*), where σ^2_{ADC} is the standard deviation in the ADC and $\sigma^2_{S_0}$ is the standard deviation

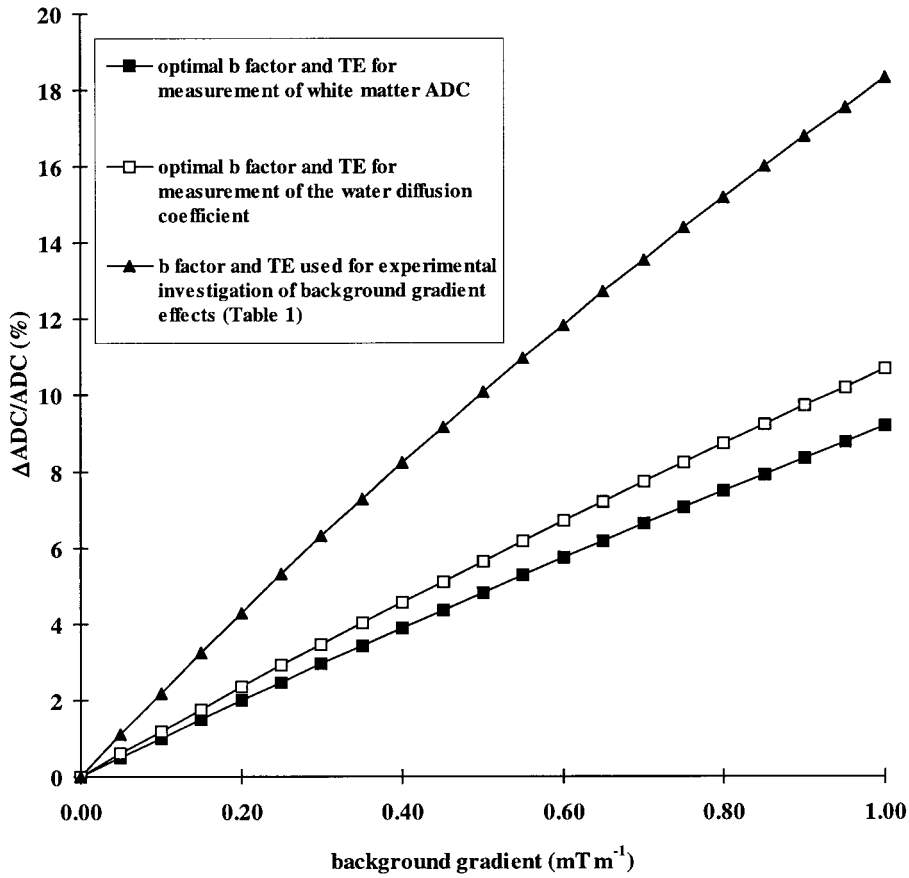

FIG. 2. Relative error in estimated ADC as a function of the component of the background gradient strength along the direction of the diffusion-sensitizing gradients in the PGSE sequence with (i) optimal *b* factor and echo time for measurement of white matter ADC, (ii) optimal *b* factor and echo time for measurement of the water diffusion coefficient, and (iii) *b* factor and echo time used for investigation of background gradient effects on measurement of white matter ADC (Table 1).

in the NMR signal in the absence of diffusion and relaxation. Assuming a signal-to-noise ratio (SNR) equal to 142 and maximal diffusion-sensitizing gradient strength of 22 mT m^{-1}, the optimal sequence parameters for estimation of water diffusion ($D = 2.2 \times 10^{-3}$ mm^2 s^{-1} (*21*), $T_2 = 2500$ ms) and white matter diffusion (ADC $= 0.71 \times 10^{-3}$ mm^2 s^{-1} (*22*), $T_2 = 72$ ms (*23*)) using the PGSE sequence are (to the nearest ms) $\delta = 25$ ms, $\Delta = 31$ ms, TE = 67 ms, $b = 491$ s mm^{-2}; and $\delta = 34$ ms, $\Delta = 40$ ms, TE = 85 ms, $b = 1148$ s mm^{-2}, respectively (*24*).

The relative error in the estimated ADC due to the noninclusion of the background and diffusion gradient cross term can be evaluated using Eq. [1] and the optimal sequence parameters for the estimation of water and white matter ADC using the PGSE sequence. In this case the additional parameters required are t_1 and t_2. Assuming that the diffusion-sensitizing gradients are placed symmetrically about the 180° pulse and neglecting the time required for the imaging gradient pulses, then $t_1 = t_2 = 5.5$ ms for water and white matter. The relative error in the estimated ADC using sequence parameters for the investigation of background gradient effects on the ADC ($\delta = 27$ ms, $\Delta = 33$ ms, TE = 117 ms, $b = 606$ s mm^{-2}) may be calculated in the same manner; in this case $t_1 = t_2 = 28.5$ ms. Figure 2 shows the relative error in ADC as a function of background gradient strength in the direction of diffusion sensitization calculated using the optimal parameters for the estimation of the water diffusion coefficient, white matter ADC, and using sequence parameters for the investigation of background gradient effects on measured brain ADC (see Table 1).

Posse (*25*) estimated the magnitude of macroscopic susceptibility gradients in the brain at 1.5 T by measuring the time shift of the echoes obtained in a gradient echo sequence and observed gradients of up to 0.16 mT m^{-1}. If these gradients are parallel or antiparallel to the direction of the diffusion-sensitizing gradients, then the relative error in the ADC based on Eqs. [1], [2], and [4] and the optimal diffusion gradient parameters for white matter is 1.8% in those regions. Repeating this calculation for a maximal gradient strength of 10 and 40 mT m^{-1}, one obtains 3.5 and 1.1%, respectively, for the relative error. For the sequence parameters used for investigation of background gradient effects (Table 1), the relative error in

TABLE 1

Imaging Parameters for Estimation of Apple Flesh and White Matter ADC (Genu of Corpus Callosum and Interface between Petrous Bone and Brain Parenchyma)

	Apple		White matter	
	PGSE	BGP	PGSE	BGP
δ (ms)	19	15	27	18
Δ (ms)	21	21	33	33
$(\Delta - \delta/3)$ (ms)	14.7	16	24	27
b (s mm^{-2})	183	249	606	606
TE (ms)	47	95	117	117
TR (ms)	5	5	2	2
Matrix	128 × 256	128 × 256	128 × 256	128 × 256
Number of acquisitions	16	16	1	1
Field of view (cm)	16	16	24	24
Slice thickness (mm)	5	5	5	5

ADC is 3.5%. It is expected, however, that the relative error in ADC is smaller in areas of the brain where susceptibility gradients are less than 0.16 mT m^{-1} and/or not along the direction of the diffusion-sensitizing gradients.

Microscopic Susceptibility-Induced Gradients

Zhong *et al.* (*26, 27*) considered the effect of microscopic susceptibility variations (such as those arising from particles of different magnetic susceptibility) on measurements of diffusion using the PGSE method. Internal gradients were considered that are not uniform, but slowly varying with position and modeled as a Gaussian distribution. This distribution was assumed to be a symmetric function, so that for each positive G_0, there is a negative G_0. A further assumption was made that the distance traveled by the diffusing molecules is small compared to the range of the gradient (the spin experiences the same gradient throughout the TE period), then the ADC measured in the presence of susceptibility variations, ADC*, was written in terms of the true ADC,

$$\mathrm{ADC}^* = \mathrm{ADC}\left[1 - \frac{1}{2}\gamma^2\Delta\sigma^2\mathrm{ADC}(\mathrm{TE} - \Delta/2)^2\right], \quad [6]$$

where σ^2 represents the variance of the internal gradients. Zhong *et al.* showed that the measured ADC* may be described as a weighted sum of ADCs from individual isochromats. ADC* for an individual isochromat may be either larger or smaller than the real ADC depending on whether the internal gradient is parallel or antiparallel to the diffusion-sensitizing gradients. For internal gradients symmetrically distributed with zero mean as described by a Gaussian distribution, the isochromats with reduced ADC have a larger signal than those with increased ADC. The higher weighting of the attenuated signal for isochromats with reduced ADC results in a reduction of the overall ADC. This reduction in ADC was experimentally verified by Zhong *et al.* in solutions containing superparamagnetic iron oxide particles. It is important to recognize from Eq. [6] that the reduction of the apparent ADC depends on Δ and thus the diffusion time, defined as $(\Delta - \delta/3)$. In this respect the behavior of the ADC in the presence of microscopic susceptibility gradients is similar to that caused by restricted or hindered diffusion. Furthermore, if the presence of significant local gradients cannot be ruled out, interpretation of diffusion time studies in terms of membrane separation and permeability is not possible. More recently Does *et al.* demonstrated that a similar reduction of the ADC is expected if the diffusing molecules experience a changing gradient during the course of the pulse sequence (*28*). In this case, however, the cross term will be reduced due to so-called motional averaging of the gradients (*29*).

Susceptibility-Induced Gradients in Human Brain

Diffusion anisotropy observed in white matter tracts has generally been attributed to the presence of cell membranes which may restrict or hinder diffusion in particular directions. However, it has also been suggested that the presence of anisotropic susceptibility-induced gradients may contribute to (*26, 27*), or be wholly responsible for (*30*), diffusion anisotropy in white matter tracts. Beaulieu and Allen (*31*) suggested that in a collection of perfectly aligned fibers, gradients may be induced through the susceptibility difference of longitudinal fiber surfaces which may be maximized by orientating the fibers perpendicularly to the B_0 field. Susceptibility gradients

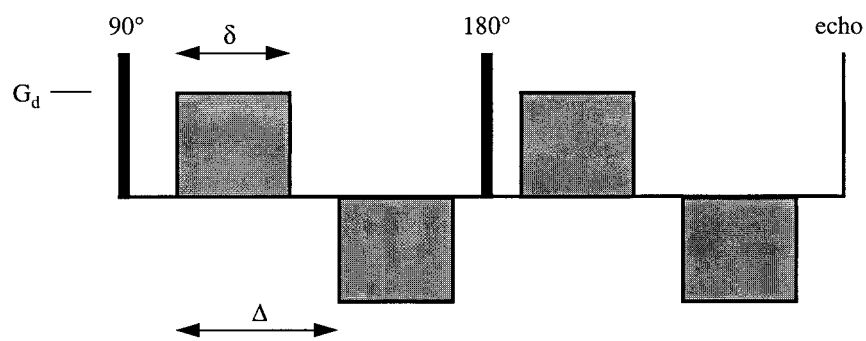

FIG. 3. The bipolar gradient pair (BGP) sequence proposed by Hong and Dixon (*36*) for the elimination of the diffusion and background gradient cross term.

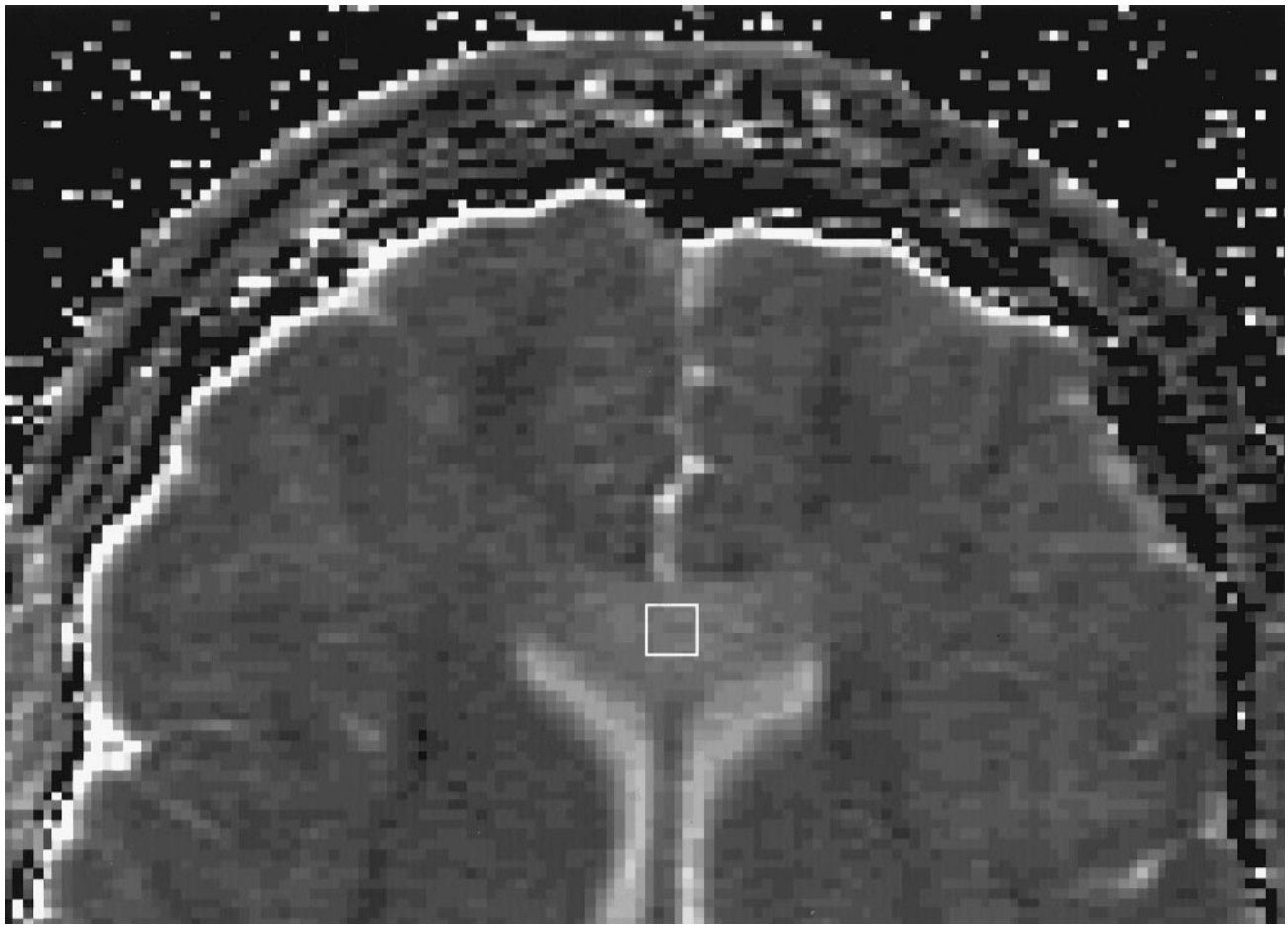

FIG. 4. Typical positioning of ROI on an ADC map for estimation of corpus callosum ADC. In this image diffusion sensitization is along the direction of the white matter fibers (right–left direction) so that the corpus callosum appears bright.

are also known to exist at interfaces between bone and tissue. The presence of a significant cross term in either case may result in a systematic error in the calculation of tissue ADC.

Rationale

The aims of this study were to (i) investigate the influence of local microscopic susceptibility gradients on the ADC (and thus diffusion anisotropy) observed in white matter tracts and (ii) to investigate the effect of known macroscopic susceptibility variations at the interface between bone and tissue on calculated ADC maps of the human brain *in vivo* using a standard clinical MRI system at 1.5 T. This can be achieved in practice by estimation of brain ADC using a pulse sequence in which the background and diffusion gradient cross term is eliminated. Comparison of results obtained where this condition is satisfied, with results obtained using the PGSE sequence (where the presence of the cross term may lead to an appreciable change in measured ADC), facilitates an evaluation of the role of susceptibility-induced gradients on the ADC, provided the diffusion time and thus restricted and hindered diffusion effects are the same for both sequences.

A number of pulse sequences have been developed to reduce or remove the effect of internal gradients. These methods are based upon the utilization of multiple refocusing RF pulses and gradient reversals in spin echo (*32, 33*) and stimulated echo sequences (*34, 35*). In this study bipolar diffusion-sensitizing gradients were positioned antisymmetrically about the 180° refocusing pulse, as shown in Fig. 3, in order to eliminate the diffusion and background gradient cross term as described previously by Hong and Dixon (*36*). In common with the terminology utilized by Hong and Dixon, we shall refer to this sequence as the bipolar gradient pair (BGP) sequence. Although we do not assume that the cross term is completely eliminated in the BGP sequence when the susceptibility gradient is varying sufficiently rapidly in space such that a diffusing spin experiences a changing gradient during TE, we shall assume that modification of the ADC under these conditions is not significant due to motional averaging of the gradient (*29*).

TABLE 2

ADC_{AP} and ADC_{RL} Corresponding to Diffusion Sensitization Perpendicular and Parallel to the Fibers of the Genu of the Corpus Callosum for Each of the Volunteers

Volunteer	$\times 10^{-3}$ mm^2 s^{-1}	PGSE	BGP	ΔADC
1	ADC_{RL}	1.72 ± 0.03	1.69 ± 0.04	0.03
1	ADC_{AP}	0.34 ± 0.02	0.36 ± 0.02	−0.02
2	ADC_{RL}	1.76 ± 0.05	1.71 ± 0.06	0.05
2	ADC_{AP}	0.57 ± 0.04	0.58 ± 0.03	−0.01
3	ADC_{RL}	1.74 ± 0.05	1.79 ± 0.05	−0.05
3	ADC_{AP}	0.54 ± 0.03	0.55 ± 0.05	−0.01

Note. The error quoted is the standard error of the mean obtained in each ROI. ΔADC is the difference between ADCs measured with the PGSE and BGP sequences and represents an estimate of the effect of the susceptibility gradients on the ADC. For each volunteer and direction of diffusion sensitization, ΔADC does not exceed the standard error of the mean of the ADC measurements. Thus, the effect of the susceptibility gradients on the ADC is considered to be not significant.

The BGP sequence was used previously by Trudeau *et al.* to study the excised spinal cord of the pig at 1.5 T (*37*) and by Beaulieu and Allen (*31*) to investigate various excised nerves of the garfish and frog at 2.35 T. In each case it was concluded that the background susceptibility-induced gradients did not contribute to the observed anisotropy. In order to conduct a study *in vivo*, however, it is necessary to circumvent the additional problem of signal modulation caused by subject motion. The navigator echo technique, which removes the phase error due to motion in each of the image echoes (*38, 39*), was employed to minimize motion artifacts in the diffusion-weighted images.

METHOD

The PGSE and BGP sequences were implemented on a whole-body 1.5 T MRI system (Signa, General Electric Medical Systems, Milwaukee, WI) equipped with actively shielded magnetic field gradients of up to 22 mT m^{-1}. A quadrature head coil was used both for RF transmission and for reception of the NMR signal. Both sequences were modified for collection of a navigator echo as described previously (*39*) but with the image echo collected prior to the navigator echo in order to maximize SNR in the image. All the experiments were performed with the diffusion-sensitizing gradients applied along the phase encode direction. This ensures that phase errors in the echoes due to rigid body translation and rotation are correctable (*39*). Shimming was performed prior to imaging and the diffusion-sensitizing gradient parameters were chosen so that the diffusion time was approximately the same for each of the sequences. For experiments performed on the human brain *in vivo* the same gradient *b* factor and echo time were used for each of the sequences to ensure that the same SNR was obtained in the diffusion-weighted images for each sequence. Cardiac gating was used and image acquisition was triggered from every second *R*-wave monitored using a pulse oximiter on the finger. Subjects were restrained using a standard chin strap and padding.

Apple Flesh

In order to investigate the effect of susceptibility variations on ADC measurements at 1.5 T, a preliminary experiment was performed on apple flesh (known to have significant local susceptibility gradients caused by small air cavities (*36*)). The imaging parameters are given in Table 1. The apple was scanned with the PGSE and BGP sequences in turn (with and without diffusion sensitization) and ADC maps were calculated from the images on a pixel-by-pixel basis by evaluating

$$\mathrm{ADC} = \frac{\ln[S(0)/S(b)]}{b_\mathrm{d}}. \qquad [7]$$

Corpus Callosum

In order to investigate the effect of possible microscopic susceptibility gradients generated in white matter tracts on ADC measurements, the corpus callosum, orientated perpendicularly to the B_0 field, was investigated. Three healthy volunteers were scanned using the PGSE and BGP sequences. The imaging parameters are given in Table 1. Axial slices through the genu of the corpus callosum were acquired with the diffusion-sensitizing gradients applied along the anterior–posterior (AP) axis and right–left axis (RL) corresponding to directions approximately perpendicular and parallel to the white matter fibers, respectively, each following an acquisition without diffusion sensitization. Diffusion-weighted images were motion artifact corrected off-line (*39*) and ADC maps were calculated as described above. Regions of interest (ROIs) were placed on the genu of the corpus callosum and mean ADC_{AP} (with sensitization along the AP axis) and mean ADC_{RL} (with sensitisation along the RL axis) over the ROI were determined for each volunteer. The values of ADC_{AP} and ADC_{RL} obtained with each of the sequences were then compared using the Mann–Whitney *U* test. Typical placement of the ROI for estimation of ADC in the corpus callosum is shown in Fig. 4.

Interface between Petrous Bone and Brain Parenchyma

An investigation of the effects of known macroscopic susceptibility variations at the interface between the petrous bone and brain parenchyma on ADC measurements was performed. This was achieved by comparing R_2' values in the brain, which are a measure of local field homogeneity, with ΔADC, the difference in the estimated ADC with and without the presence of the diffusion and background gradient cross term. If background gradients significantly alter the estimation of the ADC using the PGSE, one would expect a correlation of these two parameters to result. Three healthy volunteers were scanned. Dual gradient echo and spin echo images were obtained with

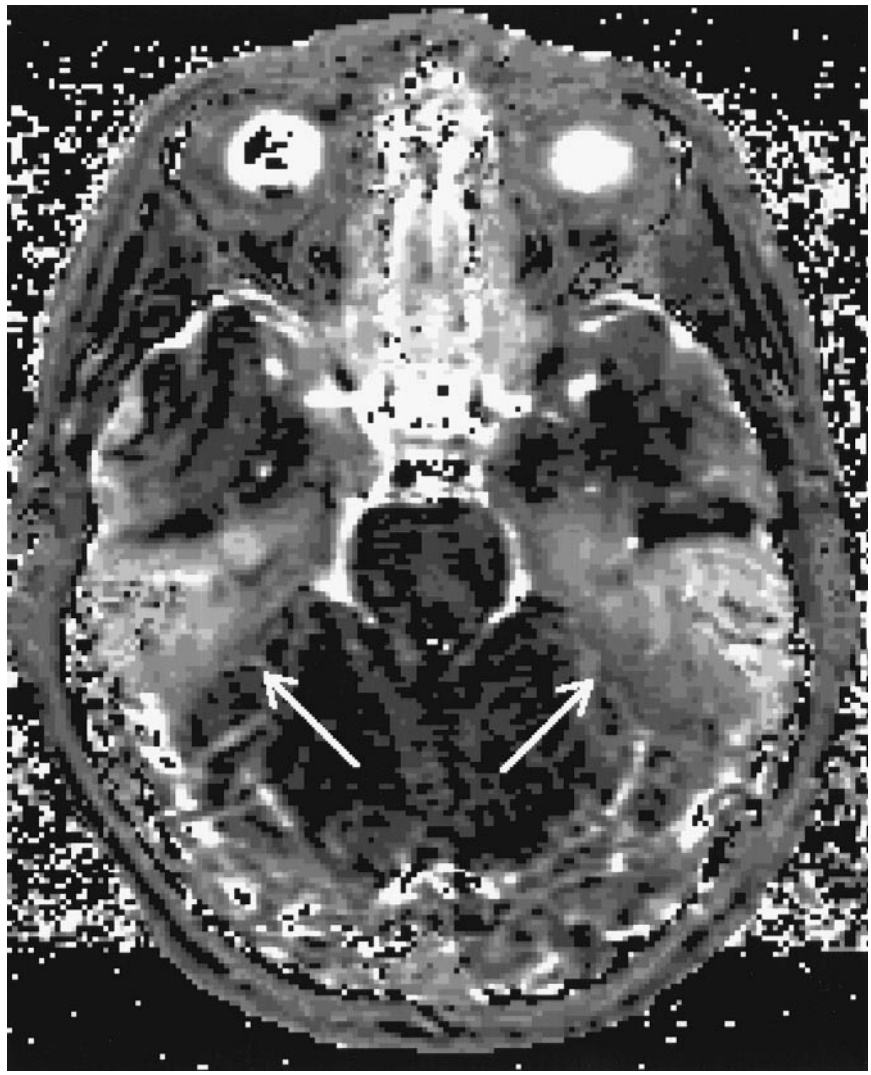

FIG. 5. R'_2 map in the axial plane through the interface between the petrous bone and brain tissue. Regions of increased R'_2 (associated with the interface) are arrowed.

slices positioned through the petrous bone. These images were used to estimate T_2^* and T_2 maps, respectively, and combined to produce R'_2 maps according to Eq. [8] in order to highlight regions of field inhomogeneity,

$$R'_2 = \frac{1}{T'_2} = \frac{1}{T_2^*} - \frac{1}{T_2}. \qquad [8]$$

Diffusion-weighted images were acquired in the axial plane, in the same slice position used for estimation of R'_2, with the PGSE and BGP sequences utilized in an identical manner to that described for the corpus callosum (see Table 1). ADC maps were calculated following navigator echo correction and then subtracted from one another to produce ΔADC maps, highlighting differences in ADC caused by background susceptibility gradients. For each volunteer seven ROIs were defined and positioned to sample evenly the range of R'_2 values in the slice. The values of ΔADC in corresponding ROIs were obtained and the relationship between R'_2 and ΔADC was examined by evaluating the Spearman rank correlation coefficient for each volunteer.

RESULTS

Apple Flesh

The ADCs of apple flesh estimated using the PGSE and BGP sequences were $(1.03 \pm 0.01) \times 10^{-3}$ mm^2 s^{-1} and $(1.52 \pm 0.01) \times 10^{-3}$ mm^2 s^{-1}, respectively (error quoted is the standard error of the mean) and found to be in good agreement with the results of Beaulieu and Allen (*31*). Using the PGSE sequence the ADC of apple flesh is underestimated by approxi-

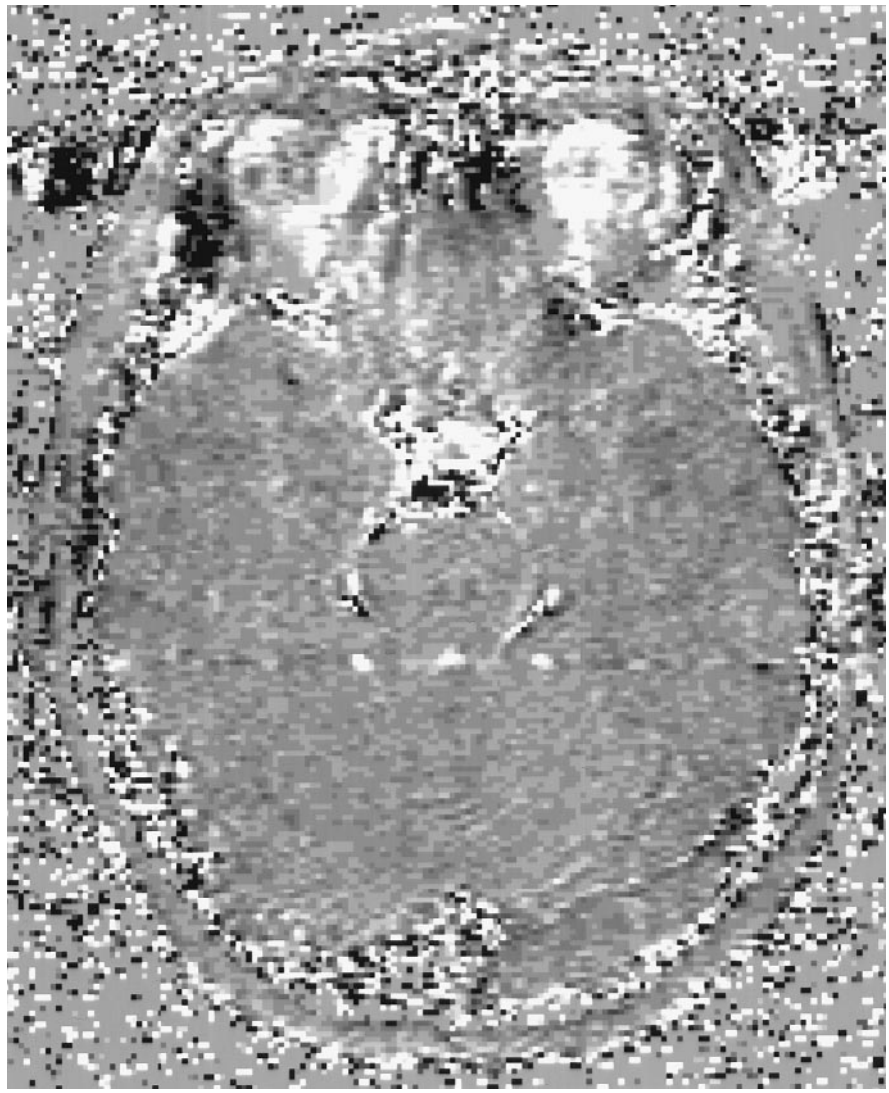

FIG. 6. ΔADC map in the axial plane through the interface between the petrous bone and brain tissue (same slice as that shown in Fig. 5).

mately 30%. Qualitatively, this underestimation is in accordance with the theory of Zhong *et al.* (*26*).

Corpus Callosum

The ADCs estimated in the genu of the corpus callosum using the PGSE and BGP sequences for each volunteer are shown in Table 2. No significant difference in ADCs obtained with the PGSE and BGP sequences in the corpus callosum was found; $P > 0.05$.

Interface between Petrous Bone and Brain Parenchyma

Typical R_2' and ΔADC maps through the petrous bone are shown in Figs. 5 and 6, respectively. The region of the petrous bone (arrowed in Fig. 5) appeared bright on the R_2' map corresponding to elevated values of R_2' compared to those in the remaining white matter. A small gray level width was used to highlight possible internal features on the ΔADC map. However, as ΔADC appeared uniform across the brain, no internal features were visible. The range of R_2' in the ROIs was 1.0–34.2 s^{-1} and the range of ΔADC in the ROIs was $\pm 0.2 \times 10^{-3}$ mm^2 s^{-1}. The largest values of ΔADC were observed at the edge of the brain, one or two pixels wide. No apparent correlation was found ($P > 0.05$) between R_2' and ΔADC in ROIs for each of the three volunteers.

DISCUSSION

The use of the navigated PGSE and BGP sequences allows a comparison of ADCs in the presence and absence of a diffusion and background gradient cross term to be made *in vivo.* The results show that at 1.5 T background gradients do not make a significant contribution to the estimated ADC and,

therefore, diffusion anisotropy observed in the white matter tracts of human brain. It is likely that at such field strengths the background gradients are too small to produce a measurable effect on the estimated ADC. This finding is compatible with the observation that the directionally averaged ADC (or mean trace of the ADT) is relatively uniform across the brain (*40*). For example, there appears to be no modification of the ADC in iron-rich regions of the brain such as the globus pallidus or in the vicinity of the sinuses, the latter of which would be expected to produce similar susceptibility gradient strengths to those encountered at the petrous bone. Indeed, theoretical calculations based on the Stejskal–Tanner formula Eq. [1] and the largest internal gradients observed by Posse (*25*) predict that the relative error in the ADC would be no greater than 1.8% when utilizing the optimal gradient *b* factor and echo time for estimation of white matter ADC. The magnitude of this error increases with decreasing maximum gradient strength. However, with a maximum gradient strength of 10 mT m^{-1}, commonly available on clinical MRI systems, this error is no greater than 3.5%. Studies of diffusion in white matter as a function of diffusion time (*41, 42*), coupled with these results, consolidate the hypothesis that restricted or hindered diffusion caused by interaction of the diffusing water molecules with the local cellular environment constitutes the major mechanism responsible for anisotropic diffusion in human brain white matter *in vivo*. The results also suggest that quantitative diffusion measurements obtained using the PGSE sequence are relatively unaffected in areas of spatially rapid changing susceptibility typically encountered in the human brain.

CONCLUSION

At 1.5 T susceptibility-induced background gradients do not make a significant contribution to human brain ADCs estimated *in vivo* using the PGSE sequence. These findings agree with those obtained on *in vitro* samples and would appear to support the hypothesis that interactions between the diffusing water molecules and the cellular environment constitute the principal mechanism for diffusion anisotropy in brain white matter at 1.5 T. This, in turn, simplifies the interpretation of diffusion time-dependent measurements in terms of membrane separation and permeability.

ACKNOWLEDGMENTS

The NMR Research Unit is funded by a generous grant from the Multiple Sclerosis Society of Great Britain and Northern Ireland. During the course of this work CAC was funded by the Brain Research Trust.

REFERENCES

1. E. O. Stejskal and J. E. Tanner, Spin diffusion measurements: Spin echoes in the presence of a time-dependent field gradient, *J. Chem. Phys.* **42,** 288–292 (1965).
2. D. Le Bihan and E. Breton, Imagerie de diffusion in vivo par resonance magnetique nucleaire, *C. R. Acad. Sci. Paris* **301,** 1109–1112 (1985).
3. D. G. Taylor and M. C. Bushell, The spatial mapping of translational diffusion coefficients by the NMR imaging technique, *Phys. Med. Biol.* **30,** 345–349 (1985).
4. K. D. Merboldt, W. Hanicke, and J. Frahm, Self-diffusion NMR imaging using stimulated echoes, *J. Magn. Reson.* **64,** 479–486 (1985).
5. M. E. Moseley, Y. Cohen, J. Kucharczyk, J. Mintorovitch, H. S. Asgari, M. Wendland, J. Tsuruda, and D. Norman, Diffusion-weighted MR imaging of anisotropic water diffusion in cat central nervous system, *Radiology* **176,** 439–445 (1990).
6. D. Chien, R. B. Buxton, K. K. Kwong, T. J. Brady, and B. R. Rosen, MR diffusion imaging of the human brain, *J. Comp. Assist. Tomogr.* **14,** 514–520 (1990).
7. M. Doran, J. V. Hajnal, N. Van Bruggen, M. D. King, I. R. Young, and G. M. Bydder, Normal and abnormal white matter tracts shown by MR imaging using directional diffusion weighted sequences, *J. Comp. Assist. Tomogr.* **14,** 685–873 (1990).
8. T. L. Chenevert, J. A. Brunberg, and J. G. Pipe, Anisotropic diffusion in human white matter: Demonstration with MR techniques in vivo, *Radiology* **177,** 401–405 (1990).
9. D. Le Bihan, E. Breton, D. Lallemand, M. Aubin, J. Vignaud, and M. Laval-Jeantet, Separation of diffusion and perfusion in intravoxel incoherent motion MR imaging, *Radiology* **168,** 497–505 (1988).
10. D. Le Bihan and R. Turner, The capillary network: A link between IVIM and classical perfusion, *Magn. Reson. Med.* **27,** 171–178 (1992).
11. P. J. Basser, D. Le Bihan, and J. Mattiello, Estimation of the effective self-diffusion tensor from the NMR spin echo, *J. Magn. Reson. B* **103,** 247–254 (1994).
12. P. J. Basser, J. Mattiello, and D. Le Bihan, MR diffusion tensor spectroscopy and imaging, *Biophys. J.* **66,** 259–267 (1994).
13. R. L. Cooper, D. B. Chang, A. C. Young, C. J. Martin, and B. Ancker-Johnson, Restricted diffusion in biophysical systems, *Biophys. J.* **14,** 161–177 (1974).
14. J. E. Tanner, Self diffusion of water in frog muscle, *Biophys. J.* **28,** 107–116 (1979).
15. J. E. Tanner, Intracellular diffusion of water, *Arch. Biochem. Biophys.* **224,** 416–428 (1983).
16. L. L. Latour, K. Svoboda, P. P. Mitra, and C. H. Sotak, Time-dependent diffusion of water in a biological model system, *Proc. Natl. Acad. Sci. USA* **91,** 1229–1233 (1994).
17. J. E. Tanner, Transient diffusion in a system partitioned by permeable barriers. Application to NMR measurements with a pulsed field gradient, *J. Chem. Phys.* **69,** 1748–1754 (1978).
18. E. Von Meerwall and R. D. Ferguson, Interpreting pulsed-gradient spin-echo diffusion experiments with permeable membranes, *J. Chem. Phys.* **74,** 6956–6959 (1981).
19. H. Y. Carr and E. M. Purcell, Effect of diffusion on free precession in nuclear magnetic resonance experiments, *Phys. Rev.* **94,** 630–638 (1954).
20. P. V. Prasad and O. Nalcioglu, A modified pulse sequence for in vivo diffusion imaging with reduced motion artifacts, *Magn. Reson. Med.* **18,** 116–131 (1991).
21. R. Mills, Self-diffusion in normal and heavy water in the range 1–45°, *J. Phys. Chem.* **77,** 685–688 (1973).
22. P. Christiensen, P. Gideon, C. Thomsen, M. Stubgaard, O. Henriksen, and H. B. W. Larsson, Increased water self-diffusion in chronic

plaques and in apparently normal white matter in patients with multiple sclerosis, *Acta Neurol. Scand.* **88,** 195–199 (1993).

23. D. H. Miller, G. Johnson, P. S. Tofts, D. MacManus, and W. I. McDonald, Precise relaxation time measurements of normal-appearing white matter in inflammatory central nervous system disease, *Magn. Reson. Med.* **11,** 331–336 (1989).

24. C. A. Clark, PhD thesis, University of London, United Kingdom (1998).

25. S. Posse, Direct imaging of magnetic field gradients by group spin-echo selection, *Magn. Reson. Med.* **25,** 12–29 (1992).

26. J. Zhong, R. P. Kennan, and J. C. Gore, Effects of susceptibility variations on NMR measurements of diffusion, *J. Magn. Reson.* **95,** 267–280 (1991).

27. J. Zhong and J. C. Gore, Studies of restricted diffusion in heterogeneous media containing variations in susceptibility, *Magn. Reson. Med.* **19,** 276–284 (1991).

28. M. D. Does, R. P. Kennan, and J. C. Gore, The ADC cross-term due to microscopic susceptibility variation. Abstracts of the International Society of Magnetic Resonance in Medicine, 6th Annual Meeting, p. 1224 (1998).

29. J. Xie, A. W. Anderson, R. P. Kennan, and J. C. Gore, q-Space measurements of the influence of microscopic field gradients on apparent diffusion. Abstracts of the Joint Meeting of the Society of Magnetic Resonance and European Society of Magnetic Resonance in Medicine and Biology, p. 916 (1995).

30. J. Lian, D. S. Williams, and I. J. Lowe, Magnetic resonance imaging of diffusion in the presence of background gradients and imaging of background gradients, *J. Magn. Reson. A* **106,** 65–74 (1994).

31. C. Beaulieu and P. S. Allen, An in vitro evaluation of the effects of local magnetic susceptibility-induced gradients on anisotropic water diffusion in nerve, *Magn. Reson. Med.* **36,** 39–44 (1996).

32. W. D. Williams, E. F. W. Seymour, and R. M. Cotts, A pulsed-gradient multiple spin-echo NMR technique for measuring diffusion in the presence of background magnetic field gradients, *J. Magn. Reson.* **31,** 271–282 (1978).

33. R. F. Karlicek and I. J. Lowe, A modified pulsed gradient technique for measuring diffusion in the presence of large background gradients, *J. Magn. Reson.* **37,** 75–91 (1980).

34. R. M. Cotts, M. J. R. Hoch, T. Sun, and J. T. Markert, Pulsed field gradient stimulated echo methods for improved NMR diffusion measurements in heterogeneous systems, *J. Magn. Reson.* **83,** 252–266 (1989).

35. L. L. Latour, L. Li, and C. Sotak, Improved PFG stimulated-echo method for the measurement of diffusion in inhomogeneous fields, *J. Magn. Reson. A* **101,** 72–77 (1993).

36. X. Hong and W. T. Dixon, Measuring diffusion in inhomogeneous systems in imaging mode using antisymmetric sensitizing gradients, *J. Magn. Reson.* **99,** 561–570 (1992).

37. J. D. Trudeau, W. T. Dixon, and J. Hawkins, The effect of inhomogeneous sample susceptibility on measured diffusion anisotropy using NMR imaging, *J. Magn. Reson. B* **108,** 22–30 (1995).

38. R. J. Ordidge, J. A. Helpern, Z. X. Qing, R. A. Knight, and V. Nagesh, Correction of motional artifacts in diffusion-weighted MR images using navigator echoes, *Magn. Reson. Imaging* **12,** 455–460 (1994).

39. A. W. Anderson and J. C. Gore, Analysis and correction of motion artifacts in diffusion weighted imaging, *Magn. Reson. Med.* **32,** 379–387 (1994).

40. C. Pierpaoli, P. Jezzard, P. J. Basser, A. Barnett, and G. Di Chiro, Diffusion tensor MR imaging of the human brain, *Radiology* **201,** 637–648 (1996).

41. M. A. Horsfield and W. I. McDonald, Restricted self-diffusion in CNS tissue by volume selective proton NMR. Abstracts of the Twelfth Meeting of the Society of Magnetic Resonance in Medicine, p. 291 (1993).

42. L. Gates and I. Cameron, Time dependence of water diffusion in human white matter. Abstracts of the Joint Meeting of the Society of Magnetic Resonance and European Society of Magnetic Resonance in Medicine and Biology, p. 355 (1995).